

Target Classification with Low-resolution Radars Based on Multifractal Correlation Characteristics in Fractional Fourier Domain

Huaxia Zhang^{1, 2} and Qiusheng Li^{1, 2, *}

Abstract—Due to the restrictions of low-resolution radar system and the influence of background clutter during the target detection, it is difficult to classify different kinds of low-resolution radar aircraft targets. In this paper, we propose a multifractal correlation method in the optimal fractional Fourier domain found by fractional Fourier transform (FrFT), in which we extract the multifractal correlation features of aircraft target echoes and do target identification combined with the support vector machine. The experimental results show that FrFT can enhance the multifractal correlation characteristics of aircraft target echoes; the multifractal correlation features extracted from the optimal fractional Fourier domain can effectively distinguish different types of aircraft; and the classification and recognition rates of the multifractal correlation method in the optimal fractional Fourier domain are higher than that of the multifractal correlation method in time domain and the multifractal method in the optimal fractional Fourier domain.

1. INTRODUCTION

Radar target classification and recognition technology plays a major role in national defense and battlefield target reconnaissance. The current development trend of radar is wideband, high-resolution, but due to its prohibitive cost, long implementation cycle and a variety of key technologies still await breakthroughs, and low-resolution radar cannot be replaced in a short term. Most air-defense radars are conventional low-resolution radars, which are mainly used for target detection and ranging. Compared with wideband radar, low-resolution radar is cheaper and more mature in technology, and many low-resolution radars operating in the VHF band have good anti-stealth and anti-radiation missile capabilities, so low-resolution radar also plays an irreplaceable role in many fields [1]. Therefore, the researches on low-resolution radar target recognition have significant strategic and practical significance, and also provide bases for researches of high-resolution radar target recognition technology [2]. Traditional low-resolution radar generally works in the high-frequency band of 3 ~ 300 MHz, with a range resolution of 300 ~ 1500 m and an azimuth resolution of 1° ~ 10°. The restrictions of low-resolution radar system and the influence of background clutter during the target detection reduce the recognition rate of surveillance radar targets, which further limits the application of aircraft [3–5]. In view of the difficulty in classifying and identifying aircraft targets with conventional low-resolution radars, many researchers have explored and obtained certain research results. Existing features for aircraft target classification include: Waveform characteristics of aircraft target echoes, amplitude modulation features, entropy in the frequency domain, ARMA (Autoregressive moving average model), dispersion situations of eigenvalue spectra, EEMD (Ensemble empirical mode decomposition), and jet engine modulation (JEM) features, among which JEM features account for the majority [6–11]. Ref. [12] analyzes the impact of observation conditions and blade overlap of the conventional low-resolution radars

Received 7 April 2019, Accepted 3 July 2019, Scheduled 23 July 2019

* Corresponding author: Qiusheng Li (bjliqiusheng@163.com).

¹ Research Center of Intelligent Control Engineering Technology, Gannan Normal University, Ganzhou, Jiangxi 341000, China. ² School of Physics and Electronic Information, Gannan Normal University, Ganzhou, Jiangxi 341000, China.

on JEM modulation characteristics in detail. The identification of low-resolution radar targets based on JEM features generally requires high pulse repetition frequency and long observation time, so it is difficult to extract the JEM characteristics of aircraft target echoes with low-resolution radar.

Fractional Fourier transform (FrFT) is an effective method to improve signal-to-noise ratio by analyzing signals in time-frequency domain with reversibility, which can be implemented by fast Fourier transform with low computational complexity [13]. FrFT is widely used in radar signal processing, such as suppression of chirp interference, SAR imaging, adaptive filtering, and detection of maritime micro-moving targets [14–17]. Du et al. introduced FrFT to extract the features of jet aircraft, propeller aircraft, and helicopters, and identified three types of aircraft targets combined with linear correlation vector machine [18]. Experiments show that this method can improve the recognition rate to a certain extent compared with traditional methods.

The aircraft target echoes of low-resolution radars and background clutter have fractal characteristics [19, 20]. Fan et al. analyzed the multifractal characteristics of AR spectra of sea clutter and detected tiny targets [21, 22]; Qu et al. classified 8 different radar signals using singular value entropy and fractal dimension [23]; Wang et al. identified jet aircraft, propeller aircraft, and helicopters with fractal dimension and normalized amplitude, with an average classification recognition rate of 92.67% [4]. Li et al. used fractal theory to study characteristics of self-affine fractal, extended fractal, and multifractal of low-resolution radar targets [24–29]; Ref. [30] analyzed the multifractal correlation characteristics of low-resolution radars in time domain and classified low-resolution radar targets by using multifractal correlation features; by analyzing the multifractal correlation characteristics of sea clutter, Guan et al. analyzed the similarity of the multifractal correlation spectra and used support vector machine for target detection [31]. FrFT can suppress clutter and facilitate signal processing, and fractal theory is an effective tool for radar target classification and identification. Combining these two methods, Gu et al. analyzed the multifractal characteristics of sea clutter in fractional Fourier domain to do moving target detection whether there is a target at sea [32]; Li et al. conducted fractal judgment and scale-free interval estimation on echoes of civil aircraft and fighters in fractional Fourier domain [33]; Zhang et al. researched multifractal characteristics of low-resolution radar target echoes in fractional Fourier domain [34].

In this paper, we propose a method, multifractal correlation analysis in fractional Fourier domain (MCIFD), to do aircraft target classification of low-resolution radars. We use FrFT to process low-resolution radar target echoes in order to decide the optimal fractional Fourier domain, in which the multifractal correlation characteristics of target echoes are studied, and multifractal correlation features are extracted to classify different types of low-resolution radar aircraft targets.

2. MULTIFRACTAL CORRELATION ANALYSIS

2.1. Fractional Fourier Transform (FrFT)

FrFT is the generalized form of Fourier transform (FT). On one hand, it has reserved the superiorities of FT; on the other hand, it has many special properties. FrFT can be viewed as a ray that transforms the signal from the time axis to the u axis by rotating the angle α counterclockwise. The p th order FrFT of the signal $f(t)$ can be defined as follows:

$$f_p(u) = \int_{-\infty}^{\infty} K_p(u, t) f(t) dt \quad (1)$$

$$k_p(t, u) = \begin{cases} A_a \exp [j\pi (u^2 \cot \alpha - 2ucsc\alpha + t^2 \cot \alpha)], & a \neq n\pi \\ \delta(t - u), & \alpha = 2n\pi \\ \delta(t - u), & \alpha = (2n + 1)\pi \end{cases} \quad (2)$$

$f_p(u)$ is the signal obtained by the p th order of FrFT in fractional Fourier domain, and $K_p(u, t)$ is the kernel function of FrFT, where $A_a = \sqrt{1 - j \cot \alpha}$, $\alpha = p\pi/2$, $p \neq 2n$, $n \in \mathcal{Z}$. Actually, in digital signal processing, we generally need the discrete form of FrFT, and this paper uses the method that transforms FrFT into a convolution form to obtain the discrete form of FrFT [34].

By using the Shannon interpolation formula:

$$f_p(u) = \sqrt{\frac{1-j\cot\alpha}{2\pi}} \exp(j\pi u^2 \cot\alpha) \times \int_{-\infty}^{\infty} [f(t) \exp(j\pi t^2 \cot\alpha) \times \exp(-j2\pi t u \csc\alpha)] dt \quad (3)$$

$$f(t) \exp(j\pi t^2 \cot\alpha) = \sum_{n=-N}^N f\left(\frac{n}{2\Delta x}\right) \exp\left[\frac{j\pi \cot\alpha n^2}{(2\Delta x)^2}\right] \times \text{sinc}\left[2\Delta x\left(t - \frac{n}{2\Delta x}\right)\right] \quad (4)$$

Substitute Eq. (4) into Eq. (3), we can yield the discrete form of FrFT:

$$f_p\left(\frac{m}{2\Delta x}\right) = \frac{A_a}{2\Delta x} \exp\left\{\frac{j\pi [\cot\alpha - \csc\alpha] m^2}{(2\Delta x)^2}\right\} \times \sum_{n=-N}^N \exp\left[\frac{j\pi (\cot\alpha)(m-n)^2}{(2\Delta x)^2}\right] \times \exp\left\{\frac{j\pi [\cot\alpha - \csc\alpha] n^2}{(2\Delta x)^2}\right\} f\left(\frac{n}{2\Delta x}\right), \quad (5)$$

where $1/\Delta x$ is the sampling interval of the time domain; n and m are the sampling points of time domain and fractional Fourier domain, respectively; N denotes the total number of time domain samples. If $f(t)$ is a linear frequency modulation signal, its FrFT $f_p(m/2\Delta x)$ forms an impulse function in the optimal fractional Fourier domain, so that the energy can be maximally aggregated.

2.2. Multifractal Theory

What multifractal theory describes is the characteristics of different levels of a factual object during the growth process. The investigated object can be divided into many small regions, whose total number is N_ε , and the size is ε ($\varepsilon < 1$) of a small region; the growth probability of the i th small region is $P_i(\varepsilon)$; and σ_i indicates the growth probabilities of different regions. The relationship between $P_i(\varepsilon)$ and ε is:

$$p_i(\varepsilon) \propto \varepsilon^{\sigma_i}, \quad i = 1, 2, \dots, N \quad (6)$$

where σ_i can be called local fractal dimension (LFD) or singular index, whose value reflects the size of growth probability of fractal in a small region. If different regions have different singular indexes, the fractal is a multifractal geometry; if all singular indexes are almost the same, the fractal can almost be considered as a monofractal geometry. Eq. (6) takes the power of q and sums to obtain the partition function:

$$\Gamma(q, \varepsilon) = \sum_{i=1}^N P_i^q(\varepsilon) = \varepsilon^{\tau(q)} \propto \sum_{i=1}^N \varepsilon^{\sigma_i q}, \quad q \in (-\infty, +\infty) \quad (7)$$

In Eq. (7), if $q \gg 1$, the subsets with large probabilities dominate; if $q \ll 1$, the subsets with small probability play a major role. In practical application, the range of q can be determined according to specific conditions. We can see from Eq. (7) that the partition function $\Gamma(q, \varepsilon)$ and ε have power-law relationship, and their slope, denoted as $\tau(q)$, is called mass index. If $\tau(q)$ is a linear function of q , the fractal has monofractal properties; if $\tau(q)$ is a convex function of q , the fractal has multifractal characteristics.

The definition of multifractal spectrum $f(\sigma)$ is the fractal dimension of fractal subsets with the same singular index. We can use the infinite sequences of $f(\sigma)$, corresponding to different σ , to represent the fractal dimension of the entire fractal in order to reflect the characteristics of the growth distribution probability.

2.3. Multifractal Correlation Theory

Based on FrFT, MCIFD discusses the multifractal correlation characteristics of aircraft target echoes of low-resolution radars and performs target recognition, which mainly involves the theoretical knowledge of FrFT, multifractal, and multifractal correlation.

Multifractal correlation theory, a generalization of multifractal theory, is generally analyzed by statistical physics. The measured distribution of multifractal geometry, whose multifractal spectra $f(\sigma)$ is $f(\sigma)$, can be described as μ , and $P_\sigma(\varepsilon)$ is the distribution probability of μ in a small region of the

multifractal geometry where the singular exponent is σ . The multifractal geometry can be divided into many small areas of size ε . The total numbers of small areas and regions, whose singular exponent is equal to σ of multifractal geometry, are denoted as N_ε and $N_\sigma(\varepsilon)$, respectively. Then, the fractal dimension D_0 defined from the perspective of measured distribution can be shown below:

$$D_0 = -\ln N_\varepsilon / \ln \varepsilon (\varepsilon \rightarrow 0) \quad (8)$$

From Eq. (8), we can get the following equation:

$$N_\varepsilon = \varepsilon^{-D_0} (\varepsilon \rightarrow 0) \quad (9)$$

D_0 denotes the fractal dimension; N_ε stands for singular exponent; and ε represents the size of small areas of multifractal geometry. Since $N_\sigma(\varepsilon) \propto \varepsilon^{-f(\sigma)} (\varepsilon \rightarrow 0)$, the probability of a specified singular exponential σ is:

$$P_\sigma(\varepsilon) = N_\sigma(\varepsilon) / N_\varepsilon \propto \varepsilon^{-D_0 - f(\sigma)} \quad (10)$$

If we set measured distribution function of multifractal geometry as $\mu_\varepsilon(x)$ under the condition that the scale is ε , the q -moment of the measured distribution is:

$$M_\varepsilon(q) = \langle \mu_\varepsilon^q(x) \rangle \propto \varepsilon^{D_0 + \tau(q)} (\varepsilon \rightarrow 0) \quad (11)$$

where $\tau(q)$ refers to a quality index; $\langle \cdot \rangle$ indicates the mathematical expectation; D_0 denotes the fractal dimension; therefore, the quality index is also called the moment index.

According to the above analysis, multifractal correlation is a generalization of multifractal, which investigates single-point statistical characteristics of measured distribution on a fractal. Multifractal correlation theory describes a probability, denoted as $P_\varepsilon(\sigma', \sigma'', d)$, in which two given singular exponents σ' and σ'' can be observed at two points on a fractal with distance d , and σ' and σ'' are both under the same scale ε , $\varepsilon < d < 1$.

Multifractal correlation spectra $\tilde{f}(\sigma', \sigma'', \omega)$ can be defined as follows:

$$P_\varepsilon(\sigma', \sigma'', d) \propto \varepsilon^{-D_0 - \tilde{f}(\sigma', \sigma'', \omega)} \quad (12)$$

$w = \ln d / \ln \varepsilon$, $P_\varepsilon(\sigma', \sigma'', d)$ stands for the multifractal correlation probability. In order to derive the relationship between multifractal correlation spectra $\tilde{f}(\sigma', \sigma'', \omega)$ and multifractal spectra $f(\sigma)$, we generalize the moment function of Eq. (11). The spatial autocorrelation function of the measured distribution $C_x(q', q'', d)$ can be defined as follows:

$$C_\varepsilon(q', q'', d) = \langle \mu_\varepsilon^{q'}(x) \cdot \mu_\varepsilon^{q''}(x+d) \rangle \propto \varepsilon^{D_0 + \tilde{\tau}(q', q'', \omega)} (\varepsilon \rightarrow 0) \quad (13)$$

$\tilde{\tau}(q', q'', \omega)$ represents the correlation moment index, and $\mu_\varepsilon(x)$ denotes the measured distribution function of multifractal geometry. Obviously, the spatial autocorrelation function $C_\varepsilon(q', q'', d)$ of the measured distribution contains more spatial information than the q -moment of the measured distribution $M_\varepsilon(q)$. Take the mathematical expectation of Eq. (13), the following formula can be deduced:

$$\langle \mu_\varepsilon^{q'}(x) \cdot \mu_\varepsilon^{q''}(x+d) \rangle \propto \varepsilon^{\tau(q') + \tau(q'') + 2D_0 + \min\{\phi(q', q''), 1\}} (\varepsilon \rightarrow 0) \quad (14)$$

$$\phi(q', q'') = \tau(q', q'') - \tau(q') + \tau(q'') - D_0 \quad (15)$$

By comparing Eq. (13) with Eq. (14), we can get the equation of correlation moment index:

$$\tilde{\tau}(q', q'', \omega) = \tau(q') + \tau(q'') + D_0 + \omega \min\{\phi(q', q''), 1\}, \quad (16)$$

where $\tau(q)$ refers to a quality index, and q' and q'' denote the moment of the measured distributions. From Eq. (16), we can conclude that the first derivative of the equation $\tilde{\tau}(q', q'', \omega)$ will produce a transition when $\phi(q', q'') = 1$, which means that the transition between two regions (I ($\phi(q', q'') < 1$) and II ($\phi(q', q'') > 1$)) is discontinuous, which is the first-order phase transition in multifractal theory.

If $\phi(q', q'') < 1$,

$$\begin{cases} \sigma' = \omega \sigma(q' + q'') + (1 - \omega) \sigma(q') \\ \sigma'' = \omega \sigma(q' + q'') + (1 - \omega) \sigma(q'') \end{cases} \quad (17)$$

else $\phi(q', q'') > 1$,

$$\begin{cases} \sigma' = \sigma(q') \\ \sigma'' = \sigma(q'') \end{cases}, \tag{18}$$

where σ' and σ'' are singular exponents. The given data, σ' , σ'' , and ω , may not satisfy both Eq. (17) and constraint $\phi(q', q'') < 1$, or Eq. (18) and constraint $\phi(q', q'') > 1$ at the same time. The point satisfying the above conditions is marked as (Q', Q'') , and the multifractal correlation spectra $\tilde{f}(\sigma', \sigma'', \omega)$ can be given by the following equation:

$$\tilde{f}(\sigma', \sigma'', \omega) = Q'\sigma' + Q''\sigma'' - \bar{\tau}(Q', Q'', \omega) \tag{19}$$

When (Q', Q'') is located in region I, multifractal correlation spectra can be obtained by substituting Eqs. (16), (17) into Eq. (19) and combining with Eq. (14).

$$\tilde{f}(\sigma', \sigma'', \omega) = \omega f[\sigma(Q' + Q'')] + (1 - \omega) \{f[\sigma(Q')] + f[\sigma(Q'')] - D_0\} \tag{20}$$

When (Q', Q'') is located in region II, multifractal correlation spectra can be obtained by substituting Eqs. (16), (18) into Eq. (19) and combining with Eq. (14).

$$\tilde{f}(\sigma', \sigma'', \omega) = f[\sigma(Q')] + f[\sigma(Q'')] - D_0 - \omega \tag{21}$$

Furthermore, the expression of probability function $P_\varepsilon(\sigma', \sigma'', d)$ can be obtained.

3. THE MULTIFRACTAL FEATURE EXTRACTION METHOD

During the short time when an aircraft is being exposed to the irradiation of the radar, the target can be viewed as a dot moving with a uniform acceleration. To simplify the description, the target classification method based on multifractal correlation features in fractional Fourier domain is referred to MCIFD. We study the implementation steps and classification performance of MCIFD algorithm.

3.1. Determination of the Optimal Fractional Fourier Domain

In the optimal fractional Fourier domain, the energy of aircraft echoes can be maximally aggregated, and the distribution of clutter is relatively dispersed, so we should find the optimal fractional Fourier domain of low-resolution radar echoes. Before feature extraction, we take FrFT to process the aircraft echoes and further confirm the optimal fractional Fourier order. In information theory, entropy can represent the average information of a signal and reflect the degree of distribution of echo energy. Renyi entropy is the generalized form of Shannon entropy, which has more generality in measuring the information. Third-order Renyi information entropy is an effective tool for measuring the information of time-frequency distribution. The maximum value of the third-order Renyi information entropy indicates that the time-frequency distribution of the analyzed signal has the highest aggregation [35]. Ref. [34] uses third-order Renyi information entropy to find the optimal fractional Fourier domain and further measures the time-frequency aggregation of the low-resolution radar target echoes. In the paper, we also use third-order Renyi information entropy to measure the aggregation performance of aircraft echoes in time-frequency domain. It is considered that the fractional Fourier domain, whose transform order is the optimal transform order p_{opr} , is the optimal fractional Fourier domain. The optimal transform order p_{opr} corresponds to the maximum value of the third-order Renyi information entropy.

The definition of third-order Renyi information entropy:

$$v = -1/2 \sum_k \log(|\text{FrFT}_P(K)|^3) \tag{22}$$

Different types of aircraft have different structural parameters, and their third-order Renyi information entropies are also different. As for the same aircraft, the third-order Renyi information entropy can also be influenced by the speed, acceleration, altitude, environment, etc. Different third-order Renyi information entropies generally have different optimal transform orders of FrFT, so every experiment needs to determine the optimal transform order of FrFT in order to achieve specific analysis of specific experiment. In order to verify the effectiveness of the algorithm, we use the measured radar echoes to carry out the following experiments. In experiment, we select six kinds of aircraft, three of which were

to fly toward the station and three to fly off the station. The radar worked in the VHF band with pulse repetition frequency of 100 Hz and pulse width of 25 μ s. Calculating the third-order Renyi information entropies of six types of aircraft respectively with the range and step of transform order p being $[0, 2]$ and 0.01, respectively, we can obtain their optimal transform orders of FrFT and further determine their optimal fractional Fourier domains. In Fig. 1, we choose two of the six types of aircraft, the first class flying toward the station and the fourth class flying off the station, to plot the third-order Renyi information entropies of target echoes. For other types of aircraft, the third-order Renyi information entropy curves are roughly similar.

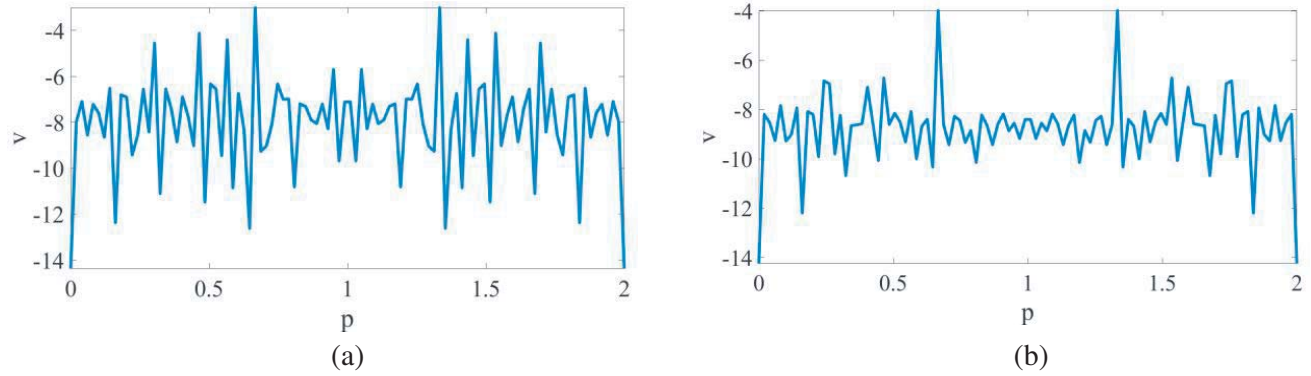


Figure 1. The third-order Renyi information entropy curve of aircraft. (a) Aircraft flying toward the station. (b) Aircraft flying off the station.

3.2. Multifractal Correlation Analysis

By using FrFT to process the original aircraft echoes and further determine the optimal transform orders, we can do multifractal correlation analysis of radar echoes in the optimal fractional Fourier domain. Multifractal correlation theory based on the multifractal theory investigates the spatial correlation of two singular exponentials, so aircraft target echoes have multifractal characteristics in the optimal fractional Fourier domain is the premise and foundation of multifractal correlation theory. Therefore, it is necessary to explore whether the aircraft target echoes have multifractal characteristics in the optimal fractional order Fourier domain. There are six types of aircraft targets, and the radar working parameters have been described above. We compare the multifractal correlation characteristics of six kinds of aircraft in time domain and the optimal fractional Fourier domain. The experimental results are shown in Figs. 2~7.

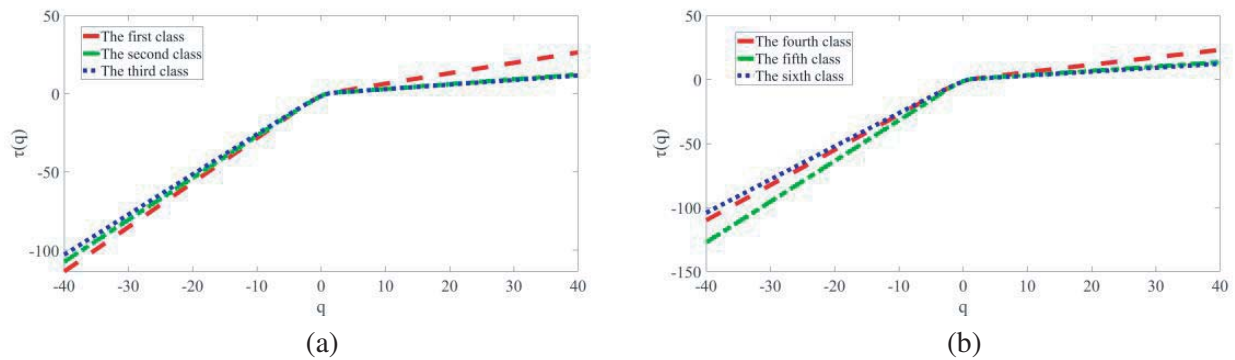


Figure 2. The mass index curves of six types of aircraft. (a) Aircraft flying toward the station. (b) Aircraft flying off the station.

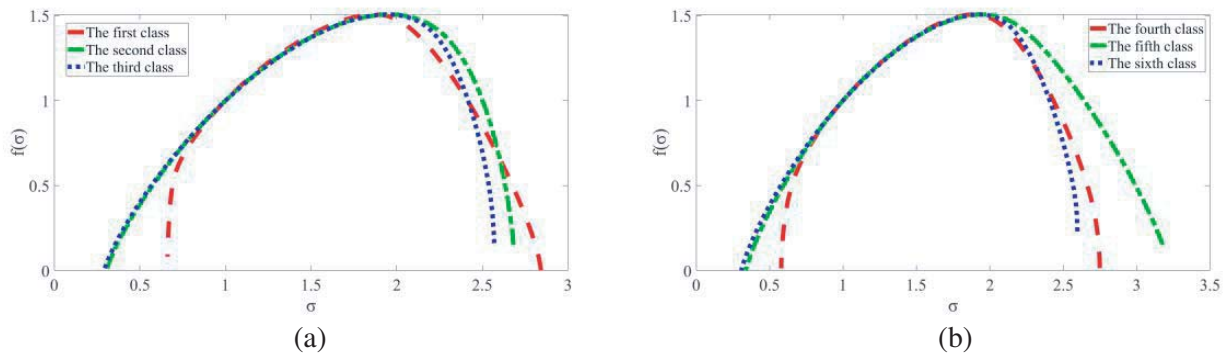


Figure 3. The multifractal spectra of six types of aircraft. (a) Aircraft flying toward the station. (b) Aircraft flying off the station.

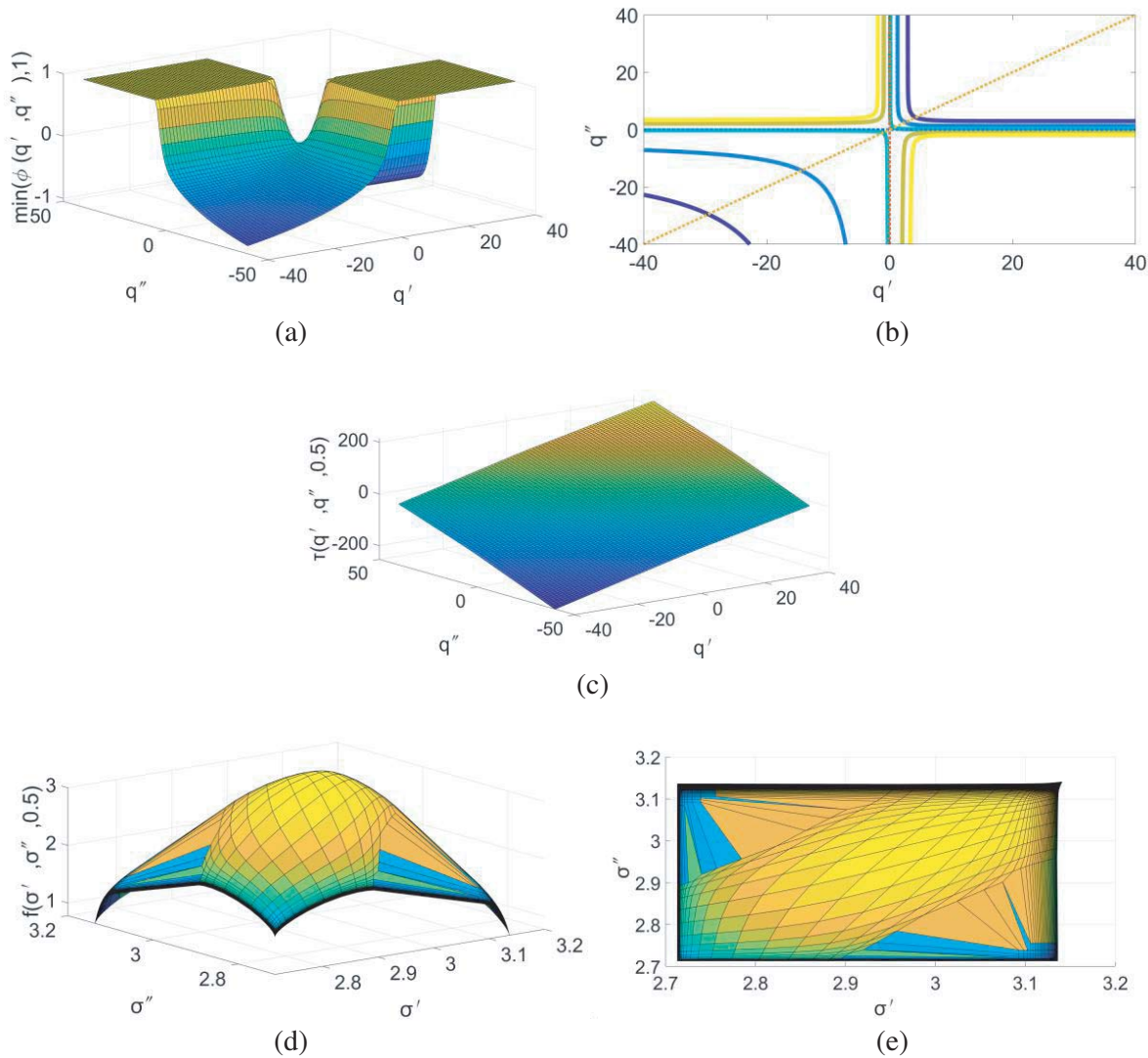


Figure 4. Multifractal correlation characteristics of aircraft flying toward station in time domain. (a) 3-D graph of $\min\{\phi(q', q''), 1\}$, (b) the contour of 3-D graph of $\min\{\phi(q', q''), 1\}$, (c) correlation moment exponents, (d) multifractal correlation spectra, (e) the contours of multifractal correlation spectra in $\sigma'-\sigma''$ plane.

We can see from Fig. 2 that the mass index curves $\tau(q)$ versus q of the six aircraft target echoes are all convex functions, which indicates that the above six types of airplane target echoes have multifractal characteristics in the optimal fractional order Fourier domain regardless of whether the aircraft are flying to station or off-station. We can also gain from Fig. 3 that the singularity indexes σ of multifractal spectra of the six kinds of aircraft target echoes have relatively large distribution ranges, and the widths of multifractal spectra are larger than 2, which verifies that the above six aircraft target echoes have multifractal characteristics in the optimal fractional Fourier domain no matter the aircraft are in toward-station or off-station state. The experiments verify that the aircraft echoes have multifractal characteristics in the optimal fractional Fourier domain, and we can explore the multifractal correlation characteristics of the aircraft echoes on this basis. The multifractal correlation characteristics of conventional radar target echoes are analyzed below.

Compared to the time domain, the shapes of 3-D graph and their contour of function $\min\{\phi(q', q''), 1\}$, shown in Figs. 4–7, change obviously in the optimal fractional Fourier domain

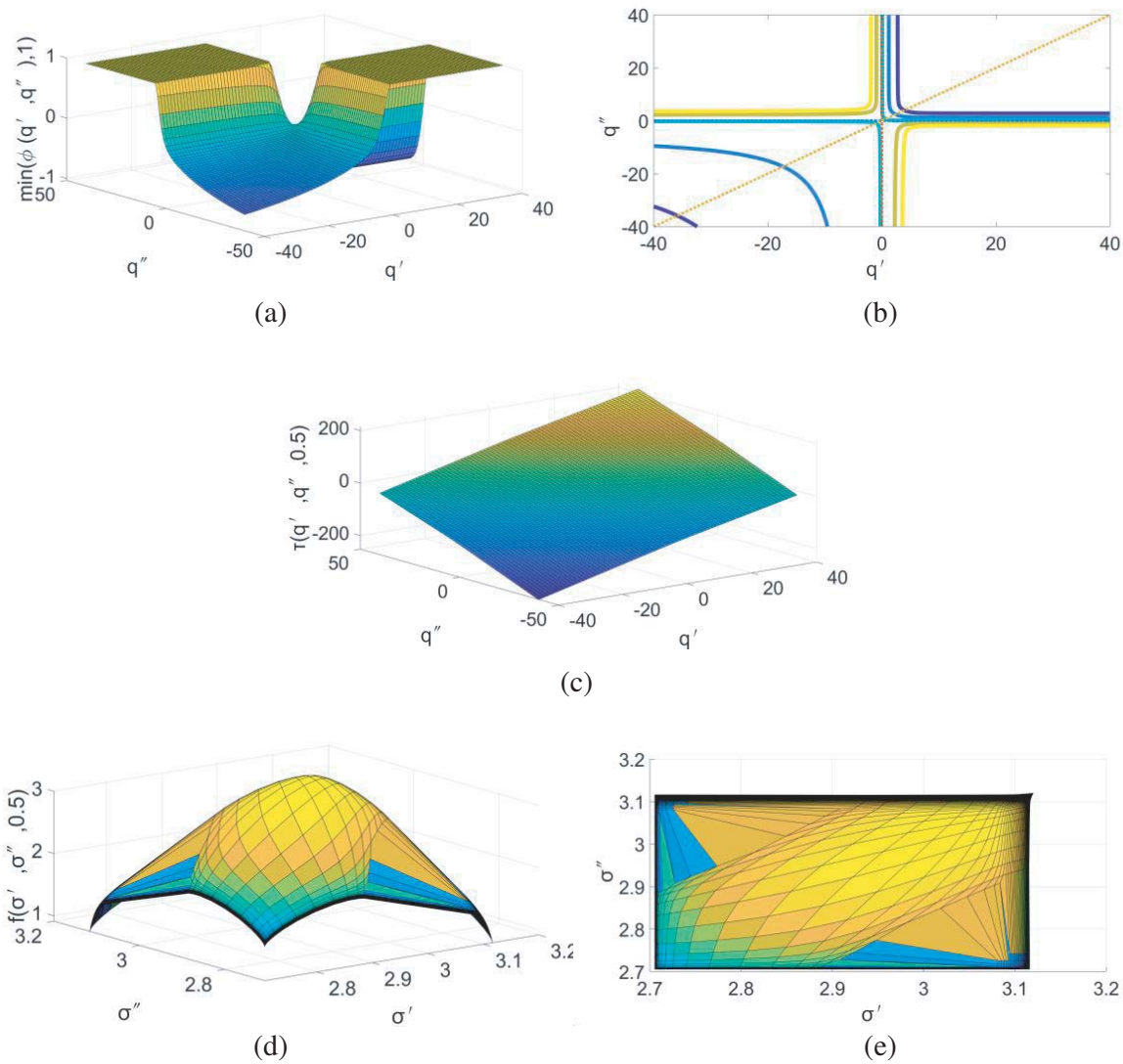


Figure 5. Multifractal correlation characteristics of aircraft flying off station in time domain. (a) 3-D graph of $\min\{\phi(q', q''), 1\}$, (b) the contour of 3-D graph of $\min\{\phi(q', q''), 1\}$, (c) correlation moment exponents, (d) multifractal correlation spectra, (e) the contours of multifractal correlation spectra in σ' - σ'' plane.

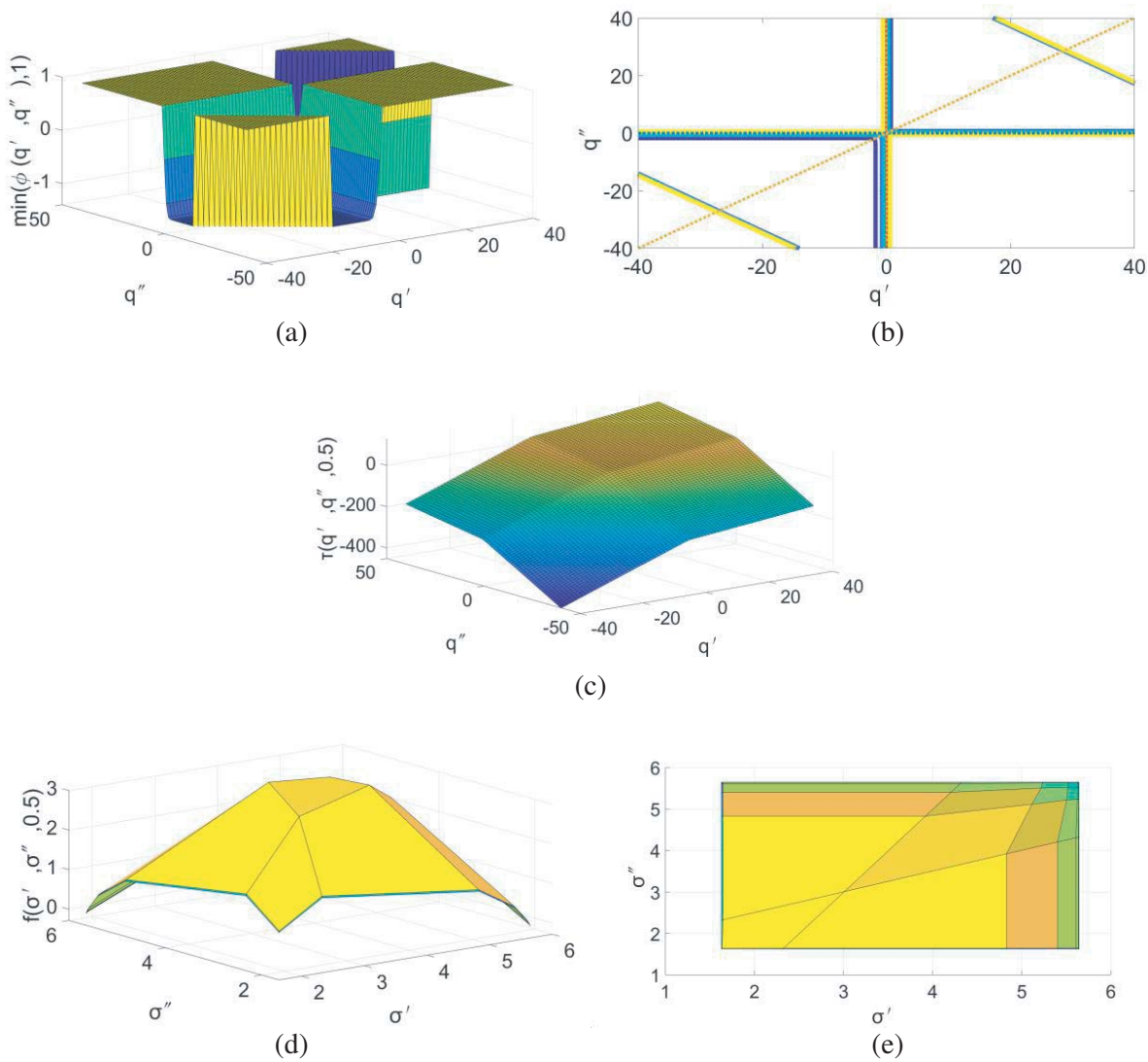


Figure 6. Multifractional correlation characteristics of aircraft flying toward station in the optimal fractional Fourier domain. (a) 3-D graph of $\min\{\phi(q', q''), 1\}$, (b) the contour of 3-D graph of $\min\{\phi(q', q''), 1\}$, (c) correlation moment exponents, (d) multifractional correlation spectra, (e) the contours of multifractional correlation spectra in σ' - σ'' plane.

regardless of whether the aircraft is flying toward the station or off-station. In the optimal fractional Fourier domain, region II ($\phi(q', q'') > 1$) increases the partial region on the basis of the area of the original region I. The graphs of correlation moment exponents are approximate planes in time domain; in the optimal fractional Fourier domain, the planes formed by the correlation moment exponents exhibit more convexity. Ref. [34] points out that FrFT can enhance the multifractal properties of low-resolution radar targets, and we can confirm that FrFT can also enhance their multifractal correlation characteristics. In the optimal fractional Fourier domain, the distribution ranges of singular exponents of multifractal correlation spectra of the above aircraft target echoes are obviously expanded, and the ranges of multifractal spectra amplitude are also increased, which further proves that the FrFT can also enhance the multifractal correlation characteristics of low-resolution radar targets.

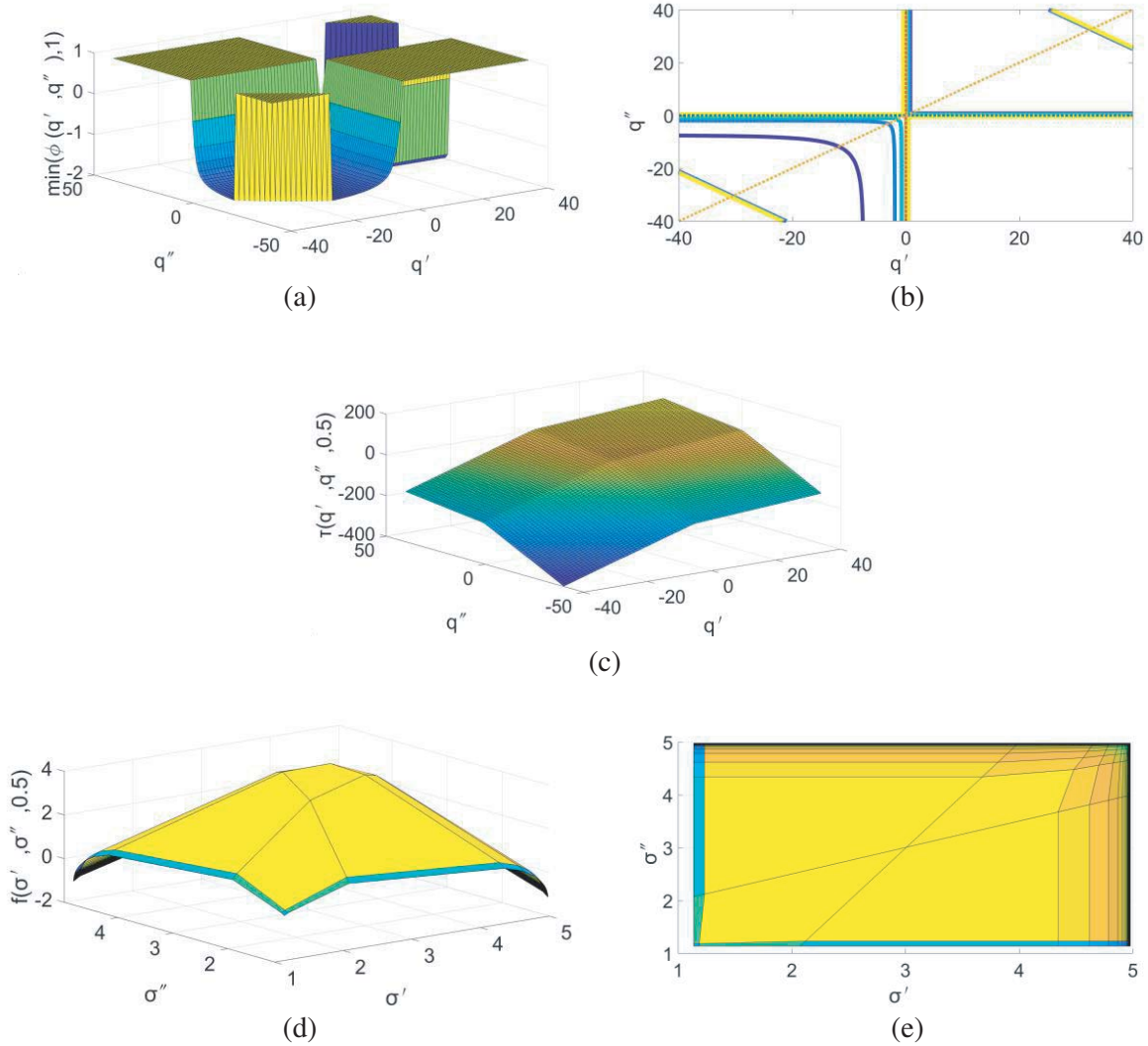


Figure 7. Multifractal correlation characteristics of aircraft flying off station in the optimal fractional Fourier domain. (a) 3-D graph of $\min\{\phi(q', q''), 1\}$, (b) the contour of 3-D graph of $\min\{\phi(q', q''), 1\}$, (c) correlation moment exponents, (d) multifractal correlation spectra, (e) the contours of multifractal correlation spectra in σ' - σ'' plane.

3.3. Extraction of Multifractal Correlation Features

Different types of aircraft targets have different physical characteristics, and their nonlinear modulations of radar echoes are also different, so the multifractal correlation spectra characteristics of target echoes of different types of aircraft are obviously different, which are undoubtedly beneficial for the classification and recognition of aircraft targets. Next, we explore the multifractal correlation spectra of aircraft target echoes and further define their characterization parameters to identify different types of aircraft targets. The characterization parameters of multifractal correlation can be defined as follows:

(1) The width of multifractal correlation spectra σ_{width}

$$\sigma_{\text{width}} = \sigma'_{\text{max}} - \sigma'_{\text{min}}, \quad (23)$$

where σ'_{max} and σ'_{min} represent the maximum and minimum values of σ' , respectively. σ_{width} can also be calculated from the range of σ'' , due to the symmetry of the multifractal correlation spectra with respect to the plane $\sigma' = \sigma''$. σ_{width} describes the association ranges of singular indexes of multifractal correlation spectra.

(2) Asymmetrical index of multifractal spectra R_σ

$$R_\sigma = \frac{\Delta\sigma_L - \Delta\sigma_R}{\Delta\sigma_L + \Delta\sigma_R}, \tag{24}$$

where $\Delta\sigma_L = \sigma_0 - \sigma_{\min}$, $\Delta\sigma_R = \sigma_{\max} - \sigma_0$, σ_0 is the singular index corresponding to the maximum of multifractal spectra $f(\sigma)$.

(3) The width of correlation moment index τ_{width}

$$\tau_{\text{width}} = \max \{ \tilde{\tau}(q', q'', \omega) \} - \min \{ \tilde{\tau}(q', q'', \omega) \} \tag{25}$$

The width of correlation moment index can measure the differences between the maximum and minimum values and describe the range of the value of the correlation moment indexes.

(4) The area of region II ($\phi(q', q'') > 1$) ϕ_{num}

$$\phi_{\text{num}} = \text{length}(\text{find}(f(q', q'') = 1)), \tag{26}$$

where $f(q', q'') = \min\{\phi(q', q''), 1\}$. Region I ($\phi(q', q'') < 1$) and region II ($\phi(q', q'') > 1$) of six kinds of low-resolution radar aircraft targets analyzed above are obviously different in time domain and optimal fractional Fourier domain, and region II has a larger area in optimal fractional Fourier domain. Therefore, a multifractal correlation parameter ϕ_{num} , which can measure the area of region II of $\min\{\phi(q', q''), 1\}$, is defined.

Figure 8~9 show the probability density distributions of four multifractal correlation parameters of six types of aircraft target echoes. The working conditions and parameters of radars have been shown above.

In the case of an aircraft flying toward the station, we can conclude from Fig. 8 that the four multifractal correlation characteristics all have strong ability for target classification. The width of multifractal correlation spectra can distinguish three types of aircraft targets easily; although the other

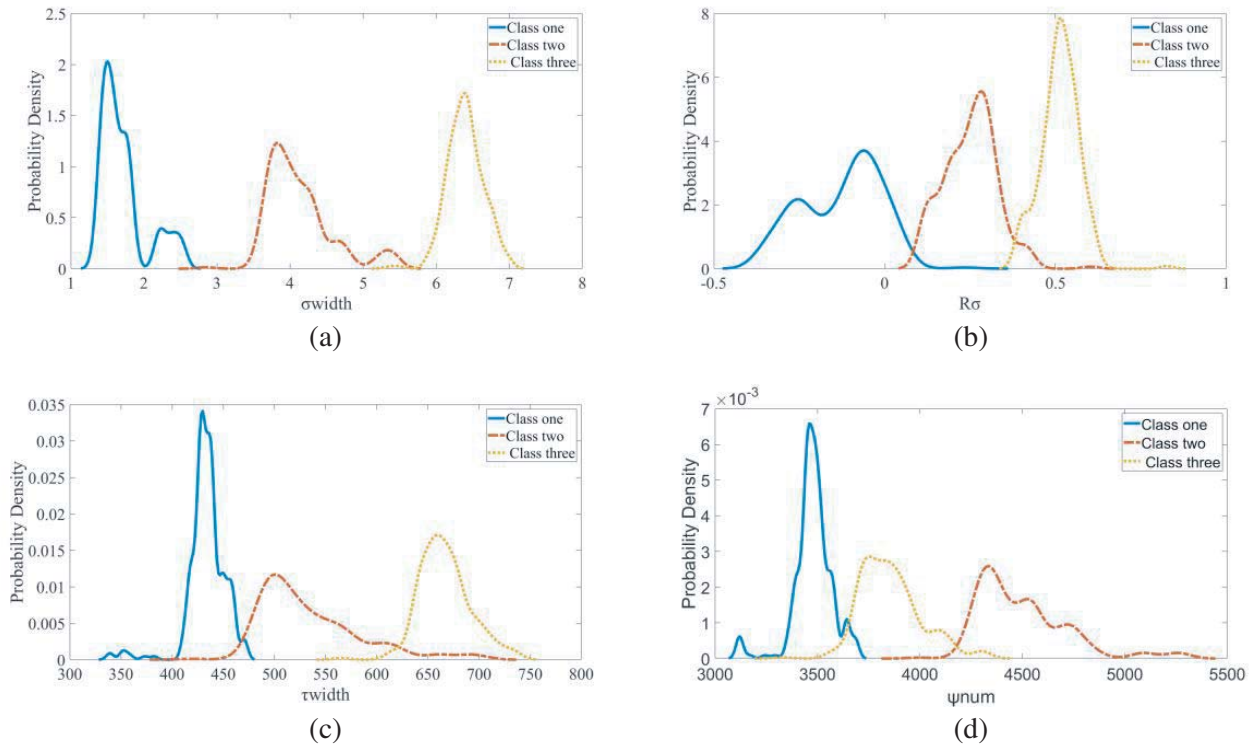


Figure 8. Probability density distributions of multifractal correlation features of aircraft flying toward station. (a) The width of multifractal correlation spectra σ_{width} , (b) asymmetrical index of multifractal spectra R_σ , (c) the width of correlation moment index τ_{width} , (d) the area of region II ϕ_{num} .

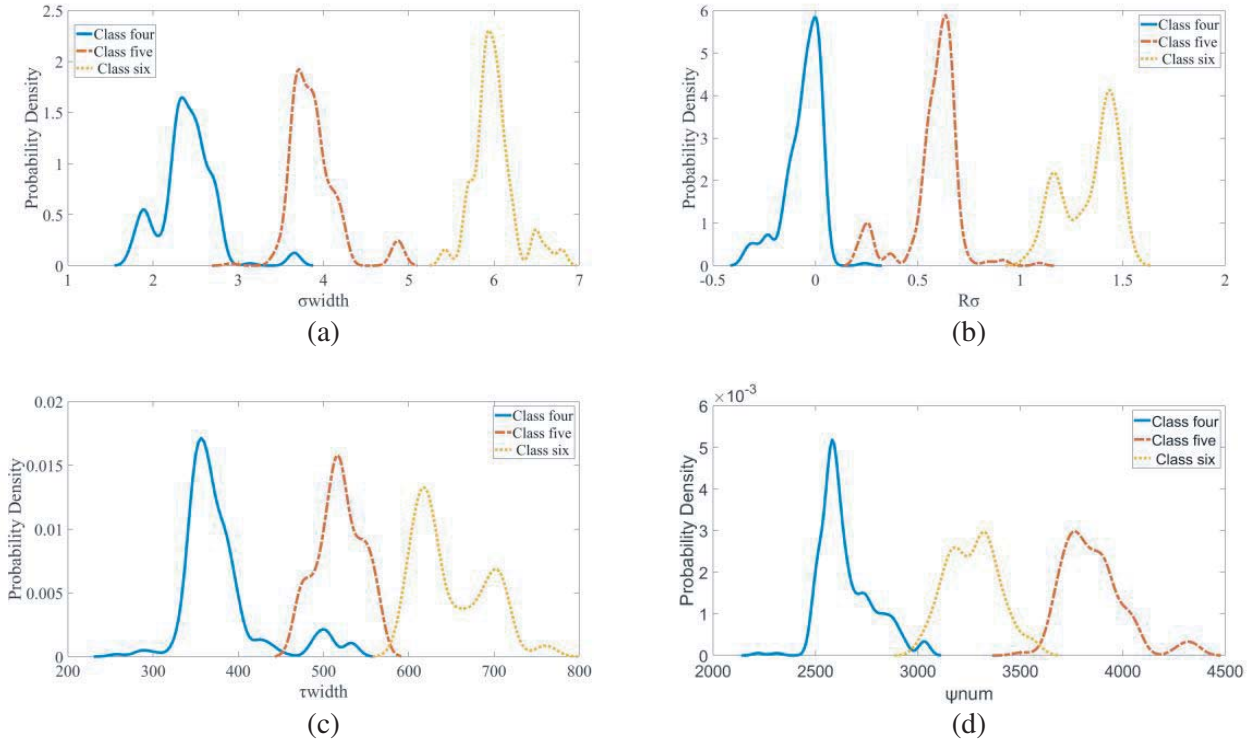


Figure 9. Probability density distributions of multifractal correlation features of aircraft flying off station. (a) The width of multifractal correlation spectra σ_{width} , (b) asymmetrical index of multifractal spectra R_{σ} , (c) the width of correlation moment index τ_{width} , (d) the area of region II ϕ_{num} .

features, asymmetrical index of multifractal spectra R_{σ} , the width of correlation moment index τ_{width} and the area of region II ϕ_{num} , overlap to a certain extent, the overlap range is small, and the probability of overlap features is small, which also has an ideal classification effect on the three types of aircraft targets.

In the case of an aircraft flying off the station, we can see from Fig. 9 that the four multifractal correlation characteristics all have strong ability for target classification. The width of multifractal correlation spectra σ_{width} and asymmetrical index of multifractal spectra R_{σ} can distinguish three types of aircraft targets easily; compared with other features, the width of correlation moment index τ_{width} overlaps more frequently. Intuitively, although the multifractal characteristics overlap within a certain range, it is hopeful to get a better performance by the comprehensive utilization of the three features.

The modulation scheme of MCIFD method can be described as follows: Firstly, we use FrFT to dispose the measured low-resolution radar target echoes; secondly, we search the optimal fractional Fourier domain of radar target echoes by third-order Renyi information entropy; thirdly, the multifractal and multifractal correlation characteristics of radar target echoes are analyzed in the optimal fractional Fourier domain, and then we extract the multifractal correlation features in order to do target classification; finally, SVM is used to identify different types of aircraft targets. Fig. 10 shows the complete signal model of the radar system.

4. CLASSIFICATION EXPERIMENTS

In this part, we experimentally study the performance of MCIFD method for aircraft target classification and recognition with the measured data. The experimental results show that the radar target correct classification rates (CCRs) based on multifractal features in time domain were higher than that of dispersion situations of eigenvalue spectra and amplitude modulation feature and frequency domain

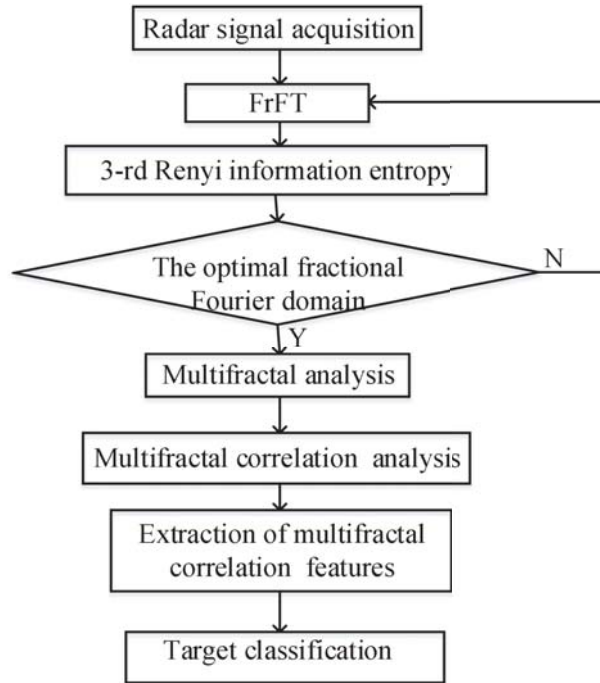


Figure 10. The complete signal model of MCIFD.

entropy [7–10]. Ref. [34] proves that the CCRs based on multifractal features extracted in the optimal fractional domain are better than that in time domain, and Ref. [30] proposes an identification method of low-resolution radar targets based on multifractal correlation in time domain. To simplify the description, the classification method described in [30] is called MFIFD, and the method proposed in [30] is called MCITD in the following text. MCITD extracts the multifractal correlation characteristics in time domain; MCIFD reveals the multifractal correlation features in the optimal fractional Fourier domain; MFIFD extracts the multifractal properties in the optimal fractional Fourier domain. We compare the classification and recognition performances among MFIFD, MCITD, and MCIFD using the measured radar target echoes that have been shown in the above experiments.

SVM has the superiorities of strong generalization ability and fast convergence speed for small, sample, and nonlinear problems, and it is widely used in radar target recognition [36]. The experiments utilize SVM as a classifier to compare the classification performances among MFIFD, MCITD, and MCIFD. The SVM classifier adopts Gaussian kernel function $K(x_i, x_j) = \exp(-\|x_i - x_j\|^2/\sigma^2)$, and we adopt reasonable parameters of Gaussian kernel function to obtain the better CCRs of aircraft targets classification in the following experiments.

In order to verify the effectiveness of the algorithm, we use the measured radar echoes to carry out the following experiments. The radar worked in the VHF band with pulse repetition frequency of 100 Hz and pulse width of 25 μ s. There are six kinds of aircraft, and each type of aircraft collects 1024 sets of echoes, of which 512 sets of data are used as training data and 512 sets of data used for testing data.

Experiment 1: Table 1 shows the CCRs of MCIFD and MFITD in the condition of aircraft flying toward the station. In the case of toward-station situation, we can conclude from Table 1 that the CCRs of MFIFD method are lower than that of MCITD method, which indicates that the multifractal correlation theory can better reflect the physical characteristics of aircraft targets than multifractal theory. Among the three kinds of aircraft target classification and recognition methods, MCIFD has the highest classification rate.

Experiment 2: Table 2 shows the CCRs of MCIFD and MFITD in the condition of aircraft flying off the station. We can conclude from Table 2 that the CCRs of MFIFD method are higher than that MCITD method, which indicates that processing the aircraft target echoes in the optimal fractional

Table 1. CCRs of MFIFD, MCITD and MCIFD with aircraft flying toward the station.

	MFIFD	MCITD	MCIFD
The first class/%	99.61	100	100
The second class/%	98.65	100	100
The third class/%	99.80	99.61	100
Average CCRs/%	99.35	99.87	100

Table 2. CCRs of MFIFD, MCITD and MCIFD with aircraft flying off the station.

	MFIFD	MCITD	MCIFD
The fourth class/%	96.65	100	100
The fifth class/%	95.18	89.51	99.22
The sixth class/%	99.61	100	100
Average CCRs/%	97.15	96.09	99.74

Fourier domain can effectively suppress the noise and improve the signal-to-noise ratio of aircraft echoes, contributing to the classification and identification of aircraft targets.

The above experiments show that MCIFD has good performance in classifying low-resolution radar targets regardless of whether the aircraft targets are in toward-station or off-station flight state. The classification performance of low-resolution radar targets based on MCIFD is better than that of MCITD, and method MCIFD analyzes the multifractal correlation characteristics of low-resolution radar aircraft targets in the optimal fractional Fourier domain. Firstly, the noise energy of radar target echoes is suppressed improving the signal-to-noise ratio in the optimal FrFT domain, which is beneficial to the classification and recognition of aircraft targets; secondly, the extracted multifractal features have strong classification ability for aircraft targets. The reason for MCIFD being superior to MFIFD is that multifractal only makes statistical analysis of singular index observed at any point on the fractal geometry support and further determines the multifractal spectra.

Multifractal correlation spectra promote the “single point” statistical characteristics to the “two points” statistical characteristics of multifractal spectra. Therefore, it can better depict the differences of physical structure of different types of aircraft targets, so the classification and recognition rates of aircraft targets are higher.

5. CONCLUSIONS

The multifractal correlation features of aircraft target echoes extracted from the optimal fractional Fourier domain provide a new method for studying the classification and recognition of low-resolution radar targets. In this paper, we use third-order Renyi information entropy to calculate the optimal fractional Fourier domain transform orders and further determine the optimal fractional Fourier domain of aircraft target echoes, in which we analyze the multifractal correlation characteristics of aircraft target echoes and further extract the multifractal correlation features to do target classification by using SVM as classifier. Experimental results show that the measured low-resolution radar target echoes have multifractal correlation characteristics on the basis of multifractal characteristics in the optimal fractional Fourier domain; compared with the multifractal correlation characteristics of aircraft target echoes in time domain, the multifractal correlation properties can be enhanced by FrFT. Regardless of whether the aircraft targets are in toward-station or off-station flight state, the correct classification and recognition rates of MCIFD are higher than that of MCITD and MFIFD. In view of the limitations of low-resolution radar system, it is only applicable to the rough target classification of conventional radars, although the CCRs have been improved.

ACKNOWLEDGMENT

Firstly, we would like to thank Professor Huang Jiang Jun at Shenzhen University for offering the experiment data. Secondly, we wish to thank the National Natural Science Foundation of China (Grant: 61561004) and the Postgraduate Innovation Fund Project of Gannan Normal University (Grant: YCX18B009) for the support to this research work. Finally we also wish to thank the anonymous reviewers for their help in improving this paper.

REFERENCES

1. Xin, Y. L. and R. C. Xu, "Research on low-resolution radar target recognition method," *Modern Electronic Technology*, Vol. 18, 17–19+22, 2005.
2. Zhang, G. W., R. D. Li, and D. Wang, "A survey of low resolution radar target classification methods," *Digital Communication World*, Vol. 5, 280, 2018.
3. Boord, W. J. and J. B. Hoffman, *Air and Missile Defense Systems Engineering*, Taylor and Francis, 2016.
4. Wang, F. Y., D. Luo, and W. H. Liu, "Research on aircraft target classification and recognition technology of low resolution airborne radar," *Journal of Radar*, Vol. 3, No. 4, 444–449, 2014.
5. Yang, S. F., H. K. Wu, X. Wang, et al., "Modulation feature extraction and classification recognition of low resolution radar targets," *Electronic Information Countermeasure Technology*, Vol. 4, 15–20, 2015.
6. Shao, Y., H. L. Wang, H. J. Zhang, et al., "Low resolution radar target recognition based on waveform characteristics," *Shipboard Electronic Countermeasure*, Vol. 38, No. 4, 62–65, 2015.
7. Song, X. J., "Research on target classification and recognition of low resolution radar," *Radar Science and Technology*, Vol. 14, No. 3, 286–290, 2016.
8. Carrière, R. and R. L. Moses, "Autoregressive moving average modeling of radar target signatures," *NASA STI/Recon Technical Report N*, Vol. 88, 225–229, 1988.
9. Chen, F., H. W. Liu, and B. Z. Du, "Target classification with low-resolution radar based on dispersion situations of eigenvalue spectra," *Science China: Information Sciences*, Vol. 53, No. 7, 1446–1460, 2010.
10. Li, Q. S. and W. X. Xie, "Air defense radar target classification method based on multifractal characteristics," *Application Research of Computers*, Vol. 30, No. 2, 405–409, 2013.
11. Li, Q., H. Zhang, Q. Lu, and L. Wei, "Research on analysis of aircraft echo characteristics and classification of targets in low-resolution radars based on EEMD," *Progress In Electromagnetics Research M*, Vol. 68, 61–68, 2018.
12. Li, Q. S., "Analysis of echo modulation characteristics of rotating components of aircraft target on conventional radar," *Journal of Chinese Academy of Sciences*, Vol. 30, No. 6, 829–838, 2013.
13. Tao, R., L. Qi, and Y. Wang, *Principle and Application of Fractional Fourier Transform*, Tsinghua University Press, 2004.
14. Xie, D. L., Z. Z. Chen, Y. M. Hong, et al., "Suppression of LFM jamming in HF ground wave radar by fractional Fourier transform," *Telecommunication Engineering*, Vol. 56, No. 3, 313–318, 2016.
15. Chen, Y., H. C. Zhao, S. Chen, et al., "Missile-borne SAR imaging algorithm based on fractional Fourier transform," *Journal of Physics*, Vol. 63, No. 10, 358–366, 2014.
16. Elgamel, S. A., C. Clemente, and J. J. Soraghan, "Radar matched filtering using the fractional Fourier transform," *IET Sensor Signal Processing for Defence*, 2010.
17. Yu, G., S.-C. Piao, and X. Han, "Fractional Fourier transform-based detection and delay time estimation of moving target in strong reverberation environment," *IET Radar, Sonar and Navigation*, Vol. 11, No. 8, 1367–1372, 2017.
18. Du, L., H. R. Shi, L. S. Li, et al., "Feature extraction method of narrowband radar aircraft target echo based on fractional-order Fourier transform," *Journal of Electronics and Information*, Vol. 38, No. 12, 3093–3099, 2016.

19. Jing, D., H. Cha, L. Zuo, et al., "Multifractal elimination trend fluctuation analysis of sea clutter," *Journal of Naval Engineering University*, Vol. 29, No. 5, 29–33, 2017.
20. Li, Q., W. Xie, and C. Luo, "Identification of aircraft targets based on multifractal spectrum features," *2012 11th International Conference on Signal Processing, ICSP 2012*, 1821–1824, Institute of Electrical and Electronics Engineers Inc., Beijing, China, October 21–25, 2012.
21. Fan, Y. F., F. Luo, M. Li, et al., "Fractal characteristics of AR spectrum expansion of sea clutter and detection of weak targets," *Journal of Xi'an University of Electronic Science and Technology (Natural Science Edition)*, Vol. 44, No. 1, 59–64, 2017.
22. Fan, Y. F., F. Luo, M. Li, et al., "Multifractal characteristics of AR spectrum of sea clutter and weak target detection method," *Journal of Electronic and Information Science*, Vol. 38, No. 2, 455–463, 2016.
23. Qu, Z. Y., X. J. Mao, and C. B. Hou, "Radar signal recognition based on singular value entropy and fractal dimension," *Systems Engineering and Electronic Technology*, Vol. 40, No. 2, 303–307, 2018.
24. Li, Q. S., X. Y. Liu, and J. P. Chen, "Fractal modeling and target classification of conventional radar aircraft echoes," *Journal of Gannan Normal University*, Vol. 36, No. 3, 34–39, 2015.
25. Li, Q. S., X. D. Yuan, and L. X. Guan, "Multifractal analysis of aircraft target echo from conventional radar," *Journal of Anhui University (Natural Science Edition)*, Vol. 36, No. 5, 47–54, 2012.
26. Li, Q., X. Xie, and Q. Lu, "Generalized dimension spectrum features based classification method for aircraft," *2016 CIE International Conference on Radar, RADAR 2016*, Institute of Electrical and Electronics Engineers Inc., Guangzhou, China, October 10–13, 2016.
27. Li, Q. S., J. H. Pei, and X. Y. Liu, "Self-affine fractal modelling of aircraft echoes from low-resolution radars," *Defence Science Journal*, Vol. 66, No. 2, 151–155, 2016.
28. Li, Q. S., W. X. Xie, and J. X. Huang, "Extended fractal characteristic analysis and target classification of air defense radar aircraft echo," *Signal Processing*, Vol. 29, No. 8, 1091–1097, 2013.
29. Li, Q., H. Zhang, and R. Lai, "Research on analysis of high-order fractal characteristics of aircraft echoes and classification of targets in low-resolution radars," *Progress In Electromagnetics Research M*, Vol. 75, 61–68, 2018.
30. Li, Q. and W. Xie, "Research on analysis of multifractal correlation characteristics of aircraft echoes and classification of targets in surveillance radars," *Progress In Electromagnetics Research B*, Vol. 54, 27–44, 2013.
31. Guan, J., N. B. Liu, J. Zhang, et al., "Multi-fractal correlation characteristics of sea clutter and weak target detection," *Journal of Electronic and Information Science*, Vol. 32, No. 1, 54–61, 2010.
32. Gu, Z. M., X. G. Zhang, and Q. Wang, "Multifractal characteristics of sea clutter and target detection in FRFT domain," *Journal of Nanjing University (Natural Science)*, Vol. 53, No. 4, 731–737, 2017.
33. Li, Q. S., X. C. Xie, H. Zhu, et al., "Fractal characteristic analysis and target classification of low resolution radar aircraft echoes in fractional fourier domain," *Application Research of Computers*, Vol. 35, No. 8, 315–318+322, 2018.
34. Zhang, H., Q. Li, C. Rong, and X. Yuan, "Target classification with low-resolution radars based on multifractal features in fractional fourier domain," *Progress In Electromagnetics Research M*, Vol. 79, 51–60, 2019.
35. Williams, W. J., M. L. Brown, and A. O. H. Iii, "Uncertainty, information, and time-frequency distributions," *Proceedings of SPIE — The International Society for Optical Engineering*, Vol. 1566, 144–156, 1991.
36. Chen, Z. R., H. Gu, W. M. Su, et al., "Improved support vector machine for low resolution radar target classification," *Systems Engineering and Electronic Technology*, Vol. 39, No. 10, 2456–2462, 2017.